Influence of Meteorology and interrelationship with greenhouse gases (CO_2 and CH_4) at a suburban site of India

Sreenivas. G, Mahesh. P*, Subin Jose, Kanchana A. L., Rao P.V.N, Dadhwal. V.K

Atmospheric and Climate Sciences Group (ACSG),

Earth and Climate Science Area (ECSA),

National Remote Sensing Center (NRSC),

Indian Space Research Organization (ISRO),

Hyderabad, India-500037

*Corresponding author: Mahesh P

Mail-Id:mahi952@gmail.com

Abstract

Atmospheric greenhouse gases (GHGs), such as carbon dioxide (CO_2) and methane (CH_4), are important climate forcing agents due to their significant impacts on the climate system. The present study brings out first continuous measurements of atmospheric GHGs using high precision LGR-GGA over Shadnagar, a suburban site of Central India during the period 2014. The annual mean CO_2 and CH_4 over the study region are found to be 394±2.92 ppm and 1.92±0.07 ppm (μ ±1σ) respectively. CO_2 and CH_4 show a significant seasonal variation during the study period with maximum (minimum) CO_2 observed during Pre-monsoon (Monsoon), while CH_4 recorded maximum during post-monsoon and minimum in monsoon. Irrespective of the seasons, consistent diurnal variations of these gases are observed. Influences of prevailing meteorology (air temperature, wind speed, wind direction and relative humidity) on GHGs have also been investigated. CO_2 and CH_4 show a strong positive correlation during winter, pre-monsoon, monsoon, and post-monsoon with correlation coefficients (Rs) equal to 0.80, 0.80, 0.61, and 0.72 respectively; indicating common anthropogenic source for these gases.Analysis of this study reveals the major sources for CO_2 are soil respiration and anthropogenic emissions while vegetation act as a main sink. Whereas the major source and sink for CH_4 are vegetation and presence of hydroxyl (OH) radicals.

Keywords: Carbon dioxide, Methane, OH radical.

1. Introduction

The Intergovernmental Panel on Climate Change (IPCC, 2013) reported that humankind is causing global warming through the emission of greenhouse gases (GHGs), particularly carbon dioxide (CO_2) and methane (CH_4).CO_2 and CH_4 concentrations have increased by 40% and 150 % respectively since pre-industrial times, mainly from fossil fuel emissions and secondarily from net land use change emissions (IPCC, 2013; Huang et al., 2015). CO_2 measurements at MaunaLoa, Hawaii (Monastersky, 2013) have exceeded the 400 ppm mark several times in May 2013. CH_4 is also receiving increasing attention due to high uncertainty in its sources and sinks (Keppler et al., 2006; Miller et al., 2007; Frankenberg et al., 2008). Stefanie Kirschke et al., (2013) reported that in India, agriculture and waste constitute the single largest regional source of CH_4. Although many sources and sinks have been identified for CH_4, their relative contribution to atmospheric CH_4 is still uncertain (A. Garg et al., 2001; StefanieKirschke et al., 2013). In India, electric power generation contributes to half of India's total CO_2 equivalent emissions (A. Garg et al., 2001).

Arid and semi-arid areas comprise about 30% of the Earth's land surface. Climate change and climate variability will likely have a significant impact on these regions (Huang et al., 2008; Huang et al., 2015). The variability of environmental factors may result in significant effects on regional climate and global climate (Wang et al., 2010), especially the radiative forcing; via the biogeochemical pathways affecting the terrestrial carbon cycle. Global climate change has serious impact on humans and ecosystems. Due to this, many factors have been identified that may reflect or cause variations in environmental change (Pielke et al., 2002). Out of these, the Normalized Difference Vegetation Index (NDVI) has become one of the most widely used indices to represent the biosphere influence on global change (Liu et al., 2011). Greenhouse and other trace gases have great importance in atmospheric chemistry and for radiation budget of the atmosphere-biosphere system (Crutzen et al., 1991). Hydroxyl radicals ($O\dot{H}$) are very reactive oxidizing agents, which are responsible for the oxidation of almost all gases that are emitted by natural and anthropogenic activities in the atmosphere. Atmospheric CO_2 measurements are very important for understanding the carbon cycle because CO_2 mixing ratios in the atmosphere are strongly affected by photosynthesis, respiration, oxidation of organic matter, biomass and fossil fuel burning, and air–sea exchange process (Machida et al., 2003).

The present study brings out first continuous measurements of atmospheric GHGs using high precision LGR-GGA over Shadnagar, a suburban site of Central India during the period 2014. In addition to GHGs observations, we have also made use of an automatic weather station (AWS) data along with model/satellite retrieved observation during the study period. Details about study area and data sets are described in the following sections.

2. Study Area

Shadnagar is situated in Mahabubnagar district of newly formed Indian state of Telangana. It is a suburban location situated ~70km away from urban site of Hyderabad (Northern side) with a population of ~0.16 million (Patil et al., 2013). A schematic map of study area is shown in Fig. 1a. Major sources of pollutants over Shadnagar can be from small and medium scale industries, biomass burning and bio-fuel as well as from domestic cooking. In the present study sampling of GHGs and related meteorological parameters are carried out in the premises of National Remote Sensing Center (NRSC), Shadnagar Campus ($17^o02'N$, $78^o11'E$). Sampling site is near (aerial distance ~ 2.25 km) to National highway 7 (NH7) and a railway track (non-electrified) is in the East (E) direction.

Mean monthly variations of temperature (°C) and relative humidity (RH %) observed at Shadnagar during 2014 are shown in Figure 1e and 1d respectively. The Indian Meteorological Department (IMD) defined monsoon as June-July-August-September (JJAS), post-monsoon (October-November-December-OND), winter (January-February-JF) and pre-monsoon (March-April-May-MAM) in India. Temperature over Shadnagar varies from ~20^oc to ~29^oc. Relative humidity (RH) in Shadnagar reached a maximum of ~82 % in monsoon from a minimum of ~48 % recorded during pre-monsoon. Surface wind speed (Fig. 1c) varies between 1.3 to 1.6 m s^{-1} with a maximum observed during monsoon and minimum in pre-monsoon. The air mass advecting (Fig. 1b) towards study site is either easterly or westerly. The easterly wind prevails during winter and gradually shifts to south-westerlies in pre-monsoon, and dominates during monsoon.

3. Data set and Methodology

Details about the instrument and data utilized are discussed in this section. The availability and frequency of the observations all data used in present study are tabulated in Table 1.

3.1 In-situ observations

3.1.1 Greenhouse Gas Analyser (GGA)

The Los Gatos Research's - Greenhouse Gas Analyser (model: LGR-GGA-24EP) is an advanced instrument capable of simultaneous measurements of CO_2, CH_4 and H_2O. This instrument is well known for high precision and accuracy which are crucial towards understanding background concentrations of atmospheric GHGs, with specifications meeting WMO standards of measurement (Berman et al., 2012; Shea et al., 2013: Mahesh et al., 2015). It is based on enhanced Off-Axis Integrated Cavity Output Spectroscopy (OA-ICOS) technology (Paul et al. 2001, Baer et al., 2002), which utilizes true wavelength scanning to record fully resolved absorption line shapes. Considering the nature of the site, flow rate is fixed to be 7 liters per minute (lpm). Ambient air entering the GGA is analysed using two near infrared (NIR) distributed feedback tunable diode lasers (TDL), one for a CO_2 absorption line near1.60 µm (ν_0= 6250 cm^{-1}) and the other to probe CH_4 and H_2O absorption lines near 1.65 µm (ν_0= 6060.60 cm^{-1}). The concentration of the gases is determined by the absorption of their respective characteristic absorption lines with a high sampling time of 1sec. A detailed explanation regarding the configuration, working and calibration procedure performed for GGA in NRSC can be found elsewhere in Mahesh et al., (2015). In the present study we used GGA retrieve CO_2 and CH_4 data. High resolution data sets are diurnally averaged and used in further analysis. Due to failure of internal central processing unit (CPU) of the analyzer, data are not recorded from pre-monsoon month of 1st May to 18th June during the study period.

3.1.2 O_3 and NO_x analyzer

Surface concentrations of O_3 and NO_X have been measured continuously using on-line analyzers (Model No.s: 49iand 42i for O_3 and NO_X respectively), procured from Thermo Scientific, USA since July 2014. The trace gases (O_3 and NOx) sampling inlet is installed on the top of a 2 m mast fixed on the roof of an 8 m high building, and ambient air flow is supplied to the instruments. The inlet prevents the ingress of rain water, and is equipped with 0.5 µm filter to prevent accumulation of dust within the instrument. The ozone analyzer is based on Beer-Lambert-Baugher law which relates absorption of light to the concentration of species as its operating principle and has an in-built calibration unit for conducting periodical span and zero checks. The NO_X analyzer utilizes a molybdenum converter to convert NO_2 into NO and estimates the NO_x

concentration by the intensity of light emitted during the chemiluminescent reaction of NO with O_3 present in the ambient air. The analyzer is integrated with zero and span calibrations which are performed twice monthly.

Simultaneous observations of meteorological parameters are obtained from an automatic weather station (AWS) installed in NRSC, Shadnagar campus as a part of Calibration and Validation (CAL/VAL) project in March 2012 is equipped with nine sensors to measure fifteen weather parameters. Weather parameters measured are at surface level and height of the AWS mast is ~10 meters. ~~Wind speed and direction measurements are collected at the maximum height (3m) and all others are at 1-1.5m height.~~

3.2 Satellite and Model observations

3.2.1 MODIS

Moderate-resolution Imaging Spectrometer (MODIS) is launched in December 1999 on the polar-orbiting NASA-EOS Terra platform (Salomonson et al. 1989; King et al. 1992). It has 36 spectral channels and acquires data in 3 spatial resolutions of 250 m, 500 m, and 1 km (channels 8–36), covering the visible, near-infrared, shortwave infrared, and thermal-infrared bands. In the present study we used monthly Normalised Difference Vegetation Index (NDVI) data obtained from Terra/MODIS at 5 km spatial resolution. The NDVI value is defined as following ratio of albedos (α) at different wavelengths:

$$\mathrm{NDVI} = \frac{\alpha_{0.86\mu m} + \alpha_{0.67\mu m}}{\alpha_{0.86\mu m} - \alpha_{0.67\mu m}} \quad (1)$$

NDVI values can range from -1.0 to 1.0 but typical ranges are from 0.1 to 0.7, with higher values associated with greater density and greenness of plant canopies. More details of the processing methods used in generating the data set can be found in James and Kalluri (1994).

3.2.2 COSMIS-RO

COSMIC (Constellation Observation System for Meteorology, Ionosphere and Climate) is a GPS (Global Positioning System) radio occultation (RO) observation system (Wang et al., 2013). It consists of six identical microsatellites, and was launched successfully on 14 April 2006. GPS radio occultation observation has the advantage of near-global coverage, all-weather capability, high vertical resolution, high accuracy and self-calibration (Yunck et al., 2000). Geophysical

parameters (such as, temperature and humidity profiles) have been simultaneously obtained from refractivity data using one-dimensional variational (1DVAR) analysis. Further COSMIC-RO profiles are used to estimate planetary boundary layer height (BLH). BLH is defined to be the height at which the vertical gradient of the refractivity or water vapor partial pressure is minimum (Ao et al., 2012), explained detail methodology for calculating the BLH from refractivity (N). The planetary boundary layer (PBL) is part of the atmosphere closest to the Earth's surface where turbulent processes often dominate the vertical redistribution of sensible heat, moisture, momentum, and aerosols/pollution (AO et al., 2012).

3.2.3 Hysplit model

The general air mass pathway reaching over Shadnagar is analysed using HYSPLIT model (Draxler and Rolph, 2003) [http://ww.arl.noaa.gov/ready/hysplit4.html]. We computed 5 day isentropic model backward air mass trajectory for all study days with each trajectory starting at 00:60 UTC and reaching study site, (Shadnagar) at different altitudes(1 km,2 km,3km and 4 km). Even though the trajectory analysis have inherent uncertainties (Stohl, 1998), they are quite useful in determining long range circulation.

4. Results and Discussion

4.1 Seasonal variations of CO_2 and CH_4

Temporal variations of CO_2 and CH_4 during the study period are shown in Figure. 2a and 2b. The circles indicate the daily mean, while triangular markers represent weakly averages and monthly mean by square markers. Annual mean of CO_2 over study region is found to be 394±2.92 (mean (μ) ± standard deviation (1σ)) ppm with an observed minimum in monsoon and maximum in pre-monsoon. Seasonal mean values of CO_2 observed during different seasons are 393±5.60, 398±7.60, 392±7.0, and 393±7.0 ppm in winter, pre-monsoon, monsoon, and post-monsoon respectively. Minimum CO_2 during winter (dry season) can be due to respiratory loss of carbon (Gilmanov et al., 2004; Aurela et al. 2004) as decreased temperature and solar radiation during this period inhibit increases in local CO_2 assimilation (Thum et al., 2009). A steady increase in CO_2 concentration is observed as season changes from winter to pre-monsoon months. Enhancement in Pre-monsoon is due to higher temperature and solar radiation prevailing during these months which stimulate the assimilation of CO_2 in the daytime and respiration in the night (Fang et al., 2014). The enhanced soil respiration during these months also compliments the

increase in CO_2 concentration during this period. In addition to these natural causes, biomass burning over Indian region can also have a significant effect on pre-monsoon CO_2 concentration. More detailed explanation of biomass burning influence on pre-monsoon GHGs concentration is discussed in section 4.6. Surface CO_2 concentration recorded a minimum during monsoon months can be mainly because of enhanced photosynthesis processes with the availability of greater soil moisture. A decrease in CO_2 concentration is also observed as the monsoon progress. The decreases in temperature (due to cloudy and overcast conditions prevailing during these months) reduce leaf and soil respiration which contributes to the enhancement of carbon uptake (Patil et al., 2013; Jing et al., 2010). Further increase during post-monsoon CO_2 is associated with high ecosystem productivity (Sharma et al., 2014) also an enhancement in soil microbial activity (Stefanie Kirschke et al., 2013).

CH_4 concentration in the troposphere is principally determined by a balance between surface emission and destruction by hydroxyl radicals (OḢ). The major sources for CH_4 in the Indian region are rice, paddies, wetlands and ruminants (Schneising et al., 2009). Annual CH_4 concentration over study area is observed to be 1.92 ± 0.07 ppm, with a maximum (2.02±0.01 ppm) observed in post-monsoon and minimum (1.85±0.03 ppm) in monsoon. Seasonal mean (average) values of CH_4 observed during different seasons are 1.93±0.05, 1.89±0.05, 1.85±0.03, and 2.02±7 ppm with respectively winter, pre-monsoon, monsoon, and post-monsoon. The highest concentration appears during post-monsoon and may be associated with the Kharif season (Goroshiet al., 2011). Hayashida et al. (2013) reported that the seasonality of CH_4 concentration over monsoon Asia is characterized by higher values in the wet season and lower values in the dry season; possibly because of the effects of strong emissions from rice paddies and wetlands during the wet season. Low mixing ratios of CH_4 observed during monsoon season were mainly due to the reduction in atmospheric hydrocarbons because of the reduced photochemical reactions and the substantial reduction in solar intensity (Abhishek Gaur et al 2014).The rate of change of CH_4 was found to be high during post-monsoon. Both biological and physical processes control the exchange of CH_4 between rice paddy fields and the atmosphere (Nishanth et al., 2014; Goroshiet al., 2011). Due to this, enhanced CH_4 observed during post-monsoon at present study area..

4.2 ***Influence of vegetation on GHGs.***

In India cropping season is classified into (i) Kharif and (ii) Rabi based on the onset of monsoon. The Kharif season is from July to October during the south-west (SW) monsoon and Rabi season is from October to March (Koshal Avadhesh, 2013). NDVI being one of the indicators of vegetation change, monthly variations of CO_2 and CH_4 against NDVI is studied to understand the impact of land use land cover on mixing ratios of CO_2 and CH_4. Monthly mean changes in NDVI, CO_2 and CH_4 are shown in Figure 2c and 2d. Monthly mean of GHGs represented in this analysis is calculated from daily mean in day time (10-16 LT). Analysis of the figure reveals that an inverse relationship exists between NDVI and CO_2; while a positive relation is observed w.r.t CH_4. Generally over this part of the country vegetation starts during the month of June with the onset of SW monsoon and as vegetation increases a decrease in CO_2 concentration is observed, due to enhancement in photosynthesis. Further a decline in NDVI is observed as the season advances from post monsoon to winter and then to pre-monsoon, and it is associated with an increase in CO_2 concentration. Similarly, the main source for CH_4 emissions are soil microbial (Stefanie Kirschke et al., 2013) activity which are more active during monsoon and post monsoon seasons.

Biomass burning (forest fire and crop residue burning) is one of the major sources of gaseous pollutants such as carbon monoxide (CO_2), methane (CH_4), nitrous oxides (NOx) and hydrocarbons in the troposphere (Crutzenet al., 1990, 1985; Sharma et al., 2010). In order to study the role of biomass burning on GHGs a case study is discussed. Figure 3c shows the spatial distribution of MODIS derived fire counts over Indian region during 14-21 April 2014 with air mass trajectories ending over study area over layed on it at different altitudes viz. 1000 m, 2000 m and 4000 m respectively. Analysis of the figure shows a number of potential fire locations on the north-western and south-eastern side of study location and trajectories indicate its possible transport to study area. Daily mean variation of GHGs during the month of Aril 2014 (Figure 3b) indicates an enhancement in GHGs during the same period (14-21 April 2014). Analysis reveals that CO_2 and CH_4 have increased by ~2% and ~0.06% respectively during event days with respect to monthly mean. This analysis reveals that long range / regional transported biomass burning have a role in enhancement of GHGs over study site. Further to understand the seasonal variation of biomass burning contribution to GHGs we analysed long term (2003-2013) Fire Energetics and Emissions Research version 1.0 (FEER v1) data over study

area. Emission coefficient (C_e) products during biomass burring is developed from coincident measurements of fire radiative power (FRP) and AOD from MODIS Aqua and Terra satellites (Ichoku and Ellison, 2014). Figure 3a shows seasonal variation of CO_2 emission due to biomass burning over the study site. Enhancement in CO_2 emission is seen during pre-monsoon months; which also supports earlier observation (Figure 2a). This analysis reveals that biomass burning has a role in pre-monsoon enhancement of CO_2 over study site. For a qualitative analysis of this long range transport, we have analysed air mass trajectories ending over study site during different seasons.

4.3 *Correlation between CO_2 and CH_4*

A correlation study is carried out between hourly averaged CO_2 and CH_4 during all season for the entire study period. The statistical analysis for different seasons is shown in Table 2. Fang et al., (2015) suggest the correlation coefficients (Rs) value higher than 0.50 indicates a similar source mechanism of CO_2 and CH_4. Also a positive correlation dominance of anthropogenic emission on carbon cycle. Our study also reveals a strong positive correlation observed between CO_2 and CH_4 during winter, pre-monsoon, monsoon, and post-monsoon with R equal to 0.80, 0.80, 0.61, and 0.72 respectively. Seasonal regression coefficients (slope) and their uncertainties (ψ_{slope}, $\psi_{y\text{-}int}$) are computed using Taylor (1997) which showed maximum during winter, pre-monsoon, and minimum in a monsoon that figure out the hourly stability of the mixing ratios between CO_2 and CH_4. This can be due to relatively simple source/sink process of CO_2 in comparison with CH_4. Figure 4 shows the seasonal variation of $\Delta CH_4/\Delta CO_2$. Dilution effects during transport of CH_4 and CO_2 can be minimized to some extent by dividing the increase of CH_4 over time by the respective increase in CO_2 (Worthy et al., 2009). In this study, background concentrations of respective GHGs are determined as mean values of the 1.25 percentile of data for monsoon, post-monsoon, pre-monsoon and winter (Pan et al., 2011; Worthy et al., 2009). Annual $\Delta CH_4/\Delta CO_2$ over the study region during the study period is found to be 7.1 (ppb/ppm). This low value clearly indicates the dominance of CO_2 over the study region. The reported $\Delta CH_4/\Delta CO_2$ values from some of the rural sites viz Canadian Arctic and Hateruma Island (China) are of the order 12.2 and ~10 ppb/ppm respectively (Worthy et al., 2009; Tohjima et al., 2014). Average $\Delta CH_4/\Delta CO_2$ ratio during winter, pre-monsoon, monsoon and post-monsoon are 9.40, 6.40, 4.40, and 8.20 ppb respectively. Monthly average, of $\Delta CH_4/\Delta CO_2$, is relatively high from late post-monsoon to

296 winter, when the biotic activity is relatively dormant (Tohjima et al., 2014). During pre-monsoon
297 decease in $\Delta CH_4/\Delta CO_2$ ratio indicates the enhancement of CO_2 relative to that of CH_4.

298

299 ***4.4 Diurnal variations of CO_2 and CH_4***

300 Figure 5a to 5d shows the seasonally averaged diurnal cycle of CO_2 and CH_4 over Shadnagar
301 during study period. The vertically bar represents the standard deviation from respective mean.
302 Irrespective of seasonal variation GHGs showed a similar diurnal variation, with maximum mixing
303 ratios observed during early morning (06:00 hrs) as well as early night hours (20:00 hrs) and
304 minimum during afternoon hours. However the difference observed in the maximum diurnal
305 amplitudes can be attributed to seasonal changes. The observed diurnal cycle of GHGs is closely
306 associated with diurnal variation of planetary boundary layer height (PBLH). For better
307 understanding of the diurnal behavior of CO_2/CH_4, we used European Centre for Medium-range
308 Weather Forecasting (ECMWF) Interim Reanalysis (ERA) PBL data set which gives the data for
309 every three hours viz. 00:00, 03:00, 06:00, 09:00, 12:00, 15:00, 18:00, and 21:00 UTC with a
310 resolution of 0.25°x0.25° (http://data-portal.ecmwf.int). Figure 5a to 5d portrays the diurnal
311 evolution of CO_2/CH_4 during different season along with the evolution of Boundary Layer Height
312 (m) on secondary y axis. The morning peak arises due to combined influence of fumigation effect,
313 (Stull 1988) and morning build-up of local anthropogenic activities (household and vehicular
314 transport). Low value of GHGs as the day progress can be attributed to increased photosynthetic
315 activity during day time and destruction of stable boundary layer and residual layer due convective
316 activity. In the evening hours, surface inversion begins and form a shallow stable boundary layer
317 (Nair et al., 2007) causing the enhancement in GHGs concentration near the surface. Similar trend
318 in diurnal variation of GHGs is reported from other parts of the country (Patil et al., 2013; Mahesh
319 et al., 2014; Sharma et al., 2014; Nishanth et al., 2014).

320 ***4.5 Influence of prevailing meteorology***

321 Redistribution (both horizontal and vertical) of GHGs also plays a role in their seasonal
322 variation, as it controls transport and diffusion of pollutants from one place to another (Hassan
323 2015). A good inverse correlation between wind speed and GHGs suggest the proximity of sources
324 near measurement site, while a not so significant correlation suggests the influence of regional

transport (Ramachandran and Rajesh, 2007). Figure 6a and 6b shows scatter plot between GHGs and wind speed during different seasons. Analysis of Figure 6 shows that there exists an inverse correlation between daily mean wind speed and GHGs. Correlation coefficients (Rs) between wind speed and CO_2 during pre-monsoon, monsoon, post-monsoon, and winter is 0.56, 0.32, 0.06, and 0.67 respectively. While for CH_4 it is found be 0.28, 0.71, 0.21, and 0.60 respectively. Negative correlation indicates that the influence of local sources on GHGs, however, poor correlation coefficients during different seasons suggest the role of regional/local transport (Mahesh et al 2014). Also an understanding of prevailing wind direction and its relationship with GHGs helps in determining their probable source regions. Table 3 shows the monthly mean variation of CO_2 and CH_4 with respect to different wind direction. Enhancement in CO_2 and CH_4 level over Shadnagar are observed to mainly come from NW and NE while the lowest is from the S and SW. This can be associated to some extend with industrial emissions located in western side of sampling site, and the influence of emission and transport from nearby urban center on the NW side of the study site.

The influence of meteorological parameters (temperature and relative humidity) on trace gases is also examined. Figure 7a and 7b (top panel corresponds to CO_2 and bottom panel represents CH_4) show the scatter plot of temperature versus relative humidity as a function of GHGs during different seasons. Daily mean data is used instead of hourly mean data, to avoid the influence of the diurnal variations on correlations. CO_2 showed a positive correlation with temperature during all season except during winter. This negative correlation can be attributed to different response of photosynthesis rate to different air temperature. IPCC (1990) reports that many mid-latitude plants shows an optimum gross photosynthesis rate when temperature varied from of 20 to 35 °C. The rate of plant respiration tends to be slow below 20°C. However, at higher temperatures, the respiration rate accelerates rapidly up to a temperature at which, it equals the rate of gross photosynthesis and there can be no net assimilation of carbon. While CH_4 showed a weak positive correlation with temperature during pre-monsoon and post-monsoon, while a weak negative correlation is observed during monsoon and winter. This could be due to the rate of chemical loss reaction with OH is faster in summer and minimum in other seasons. A case study on CH_4 sink mechanism has discussed in section 4.6. Seasonal variation of GHGs also showed an insignificantly negative correlation with relative humidity. One of the supporting argument can be in humid conditions, these stoma can fully open to increase the uptake of CO_2 without a net water

loss. Also, wetter soils can promote decomposition of dead plant materials, releasing natural fertilizers that help plants grow (Abhishek et al., 2014).

Figure 8a and 8b illustrates the daily mean variation of GHGs with respect to soil moisture and soil temperature (Top panel represent the seasonal variation of CO_2 w.r.t soil moisture and soil temperature, while bottom panel represent the seasonal variation of CH_4 against the same parameters). It's quite interesting to observe that GHGs behave differently w.r.t soil moisture during different seasons. CH_4 shows a positive relationship during monsoon and post-monsoon and an inverse relationship exist during pre-monsoon and winter; while a reverse relationship exist for CO_2. During wet season aeration is restricted (Smith et al. 2003) hence soil respiration is limited, which decrease CO_2 flux. This can be one of the factors for low values of CO_2 during monsoon months, during dry months soil may act as sink of CH.

4.5.1 Influence of boundary layer height on GHGs mixing ratios

The planetary boundary layer is the lowest layer of the troposphere where wind speed as a function of temperature plays major role in its thickness variation. It is an important parameter for controlling the observed diurnal variations and potentially masking the emissions signal (Newman et al., 2013). Since complete set of COSMIC RO data is not available during the study period, in this analysis we have analysed RO data from July 2013 to June 2014, along with simultaneous observations of GHGs. Monthly variations (Figure not show) of BLH computed from high vertical resolution of COSMIC-RO data against CO_2 and CH_4 concentrations. Monthly BLH is observed to be minimum (maximum) during winter and monsoon (pre monsoon) seasons and it closely resembles with the air temperature pattern. The highest (lowest) BLH over study region was identified 3.20 km (1.50 km). A monthly average air temperature is maximum (minimum) of 29°C (20°C) during the summer (winter) months.

Seasonal BLH during winter, pre-monsoon, monsoon and post monsoon are 2.10 km, 3.15 km, 1.74 km and 2.30 km respectively. Its influence on CO_2 and CH_4 mixing ratios are shown in Figure 9a and 9b. X axis represents the seasonal transition i.e. monsoon to post monsoon (M-PM) etc and y axis indicates seasonal difference of BLH and GHGs concentration respectively. As seasonal BLH increase, mixing ratios of CO_2 (CH_4) decreased from 8.68 ppm to 5.86 ppm (110 ppb to 40 ppb). This effect clearly captured by seasonal diurnal averaged BLH data sets used from ECMWF-

ERA. The amount of biosphere emissions influence on CO_2 and CH_4 can be estimated through atmospheric boundary layer processes. Since the study region being a flat terrain, variations in CO_2 and CH_4 were mostly influenced by BLH through convection and biosphere activities.

4.6 Methane (CH_4) sink mechanism

Methane (CH_4) is the most powerful greenhouse gas after CO_2 in the atmosphere due to its strong positive radiative forcing (IPCC, AR5). Atmospheric CH_4 is mainly (70-80%) from biological origin produced in anoxic environments, by anaerobic digestion of organic matter (Crutzen and Zimmermann, 1991). The major CH_4 sink is oxidation by hydroxyl radicals (OH), which accounts for 90 % of CH_4 sink (Vaghjiani and Ravishankara, 1991; Kim et al., 2015). OH radicals are very reactive and are responsible for the oxidation of almost all gases in the atmosphere. Primary source for OH radical formation in the atmosphere is photolysis of ozone (O_3) and water vapor (H_2O). Eisele et al., (1997) defined primary and secondary source of OH radicals in the atmosphere. Primary source of OH radical is as follows;

$$O_3 + hv\ (\lambda \leq 310\ nm) \rightarrow O_2 + O(^1D) - - - (2)$$

$$where O(^1D)\ is\ electronically\ excited\ atom$$

$$O(^1D) + O_2 \rightarrow O + M - - - (3)$$

$$O(^1D) + H_2O \rightarrow 2OH - - - (4)\ \ primary\ OH\ formation$$

Removal of CH_4 is constrained by the presence of OH radicals in the atmosphere. A 1 min time series analysis of CH_4, NO_x, O_3 and H_2O and associated wind vector for August 2014 to understand the CH_4 chemistry is shown in Figure 10a and Figure 10b. Low NO_x (1-2 ppb) values are shown in horizontal elliptical region of Figure 10a and observed corresponding low CH_4 (1.80 ppm) concentrations. The low NO_x in turn produces high OH radicals in the atmosphere due to conversion of HO_2 radical by NO, which removes CH_4 through oxidation process as shown below.

$$HO_2 + NO \rightarrow O\dot{H} + NO_2 - - - (5)\ when\ NO_x\ levels\ 1 - 2\ ppb$$

$$CH_4 + O\dot{H} \rightarrow C\dot{H}_3 + H_2O - - - (6)\ \ main\ CH_4\ removal\ process$$

$$NO_2 + OH + M \rightarrow HNO_3 + M - - - (7) \text{ if } NO_x > 2\ ppb\ (OH \downarrow, CH_4 \uparrow)$$

Crutzen and Zimmermann, (1991) and Eisele et al., (1997) observed that at low NO_x (0.5-2.0 ppb) levels most HO_x family radicals such as HO_2 and peroxy radicals (RO_2) react with NO to form OH radicals. Therefore OH radicals are much higher in the case of low NO_x. When NO_x levels increase more than 2 ppb, most of the OH radicals react with NO_2 to form nitric acid (HNO_3). In first order, the levels of CH_4 in the atmosphere depend on the levels of NO_x though the production of OH radicals in the atmosphere is still uncertain. Figure 10a and 10b showed high CH_4, H_2O, O_3 and NO_x during a few days in August 2014. High concentrations of CH_4, NO_x and other gases are observed in the eastern direction of study site. Very high NO_x levels above 10 ppb are observed and subsequently CH_4 concentrations also increased to 2.40 ppm from 1.80 ppm. In the eastern direction of study site a national highway and single line broad gauge railway network are present which act as possible sources of NOx, CH_4 and CO_2. Increase in emissions of NO_x causes decline in the levels of OH radicals and subsequently observed high CH_4 over the study region.

4.7 Long range circulations

To understand the role of long range circulation, we separated the trajectory into 4 clusters based on their pathway, namely North-East (N-E), North-West (N-W), South-East (S-E), South-West (S-W). The main criterion of trajectory clustering is to minimize the variability among trajectories and maximize variability among clusters. Cluster mean trajectories of air mass and their percentage contribution to the total calculated for each season over the study period at 3 Km altitude are depicted in Figure 11. Majority of air mass trajectories during winter (~44%), pre-monsoon (~64%), monsoon (~80%) and post-monsoon (~41%) are originating from NW parts of the study site. For a comprehensive analysis, percentage occurrences of cluster mean trajectories of air mass over study area during different season at different altitudes are also tabulated in Table 4. During post-monsoon to early pre-monsoon periods which are generally the post-harvest period for some of the crops agriculture residue burning which are quite common in the NW and NE regions part of India (Sharma et al, 2010).Our analysis reveals that during this period majority of air mass reaching the study site at different altitudes come from this part of the country.

5. Conclusions

The present study analysed the seasonal variations of atmospheric GHGs (CO_2 and CH_4) and associated prevailing meteorology over Shadnagar, a suburban site of Central India during the period 2014. The salient findings of the study are the following:

- Irrespective of seasons, major sources for CO_2 are soil respiration and anthropogenic emissions while vegetation acts as a main sink. Whereas the major source and sink for CH_4 are vegetation and presence of hydroxyl (OH) radicals. In addition, boundary layer dyanamics and long range transport also plays a vital role on GHGs mixing ratios.
- The annual mean of CO_2 and CH_4 over the study region are found to be 394±2.92 ppm and 1.92±0.07 ppm ($\mu \pm 1\sigma$) respectively. CO_2 and CH_4 show a significant seasonal variation during the study period. Maximum (Minimum) CO_2 is observed during Pre-monsoon (Monsoon), while CH_4 recorded maximum during post-monsoon and minimum in monsoon. Seasonal analysis of FEER data also showed maximum emission of CO_2 due to biomass burning during pre-monsoon months which indicates the influence of biomass burning on local emissions.
- CO_2 and CH_4 showed consistent diurnal behavior in spite of their significant seasonal variations, with an observed morning (06:00 IST) maxima, followed by afternoon minima (14:00 IST) and enhancing in the late evening (~22:00 IST).
- Correlation coefficient (Rs) between wind speed and CO_2 during pre-monsoon, monsoon, post-monsoon and winter is 0.56, 0.32, 0.06 and 0.67 respectively. While for CH_4 it is found be 0.28, 0.71, 0.21, and 0.60 respectively. Negative correlation indicates that the influence of local sources on GHGs, however, poor correlation coefficients during different seasons suggest the role of regional/local transport.
- CO_2 showed a positive correlation with temperature during all seasons except during winter. Whereas CH_4 showed a weak positive correlation with temperature during pre-monsoon and post-monsoon, while showing a weak negative correlation during monsoon and winter.
- CO_2 and CH_4 showed a strong positive correlation during winter, pre-monsoon, monsoon and post-monsoon with Rs equal to 0.80, 0.80, 0.61 and 0.72 respectively. This clearly indicates common anthropogenic sources for these gases.

Acknowledgment

This work was part of the Atmospheric CO_2 Retrieval and Monitoring (ACRM) under National Carbon Project (NCP) of ISRO-GBP. Authors sincerely acknowledge Mr. Biswadip Gharai, ACSG/ECSA for providing LULC data and to Mr. Mallikarjun, ACSG/ECSA for his support in data collection. We thank D & PQE division of NRSC and Mrs. Sujatha P, ACSG for sharing AWS and boundary layer data. The authors are grateful to the AT-CTM project of ISRO-GBP for providing the O_3 and NO_x analyzers. We would also like to thank HYSPLIT, ECMWF-ERA, MODIS and COSMIC team for providing scientific data sets used in this study. We also thankful to anonymous referees and the editor for providing constructive suggestions which certainly improved the quality of manuscript.

References

Ao, C. O., Waliser, D. E., Chan, S. K., Li, J. L., Tian, B., Xie, F., & Mannucci, A. J. Planetary boundary layer heights from GPS radio occultation refractivity and humidity profiles. Journal of Geophysical Research: Atmospheres (1984–2012), 117(D16), (2012).

Aurela M, Lohila A, Tuovinen JP, Hatakka J, Riutta T, Laurila T (2009) Carbon dioxide exchange on a northern boreal fen. Boreal Environment Research 14(4): 699-710

Baer, D. S., Paul, J. B., Gupta, M., & O'Keefe, A. Sensitive absorption measurements in the near-infrared region using off-axis integrated cavity output spectroscopy. In International Symposium on Optical Science and Technology (pp. 167-176). International Society for Optics and Photonics, (2002).

Berman, E. S., Fladeland, M., Liem, J., Kolyer, R., & Gupta, M. Greenhouse gas analyzer for measurements of carbon dioxide, methane, and water vapor aboard an unmanned aerial vehicle. Sensors and Actuators B: Chemical, 169, 128-135, (2012).

Chen, H., Wu, N., Wang, Y, & Peng, C. Methane is an Important Greenhouse Gas. Methane Emissions from Unique Wetlands in China: Case Studies, Meta Analyses and Modelling, chapter 1, (2015).

Crutzen, P. J., & Andreae, M. O. Biomass burning in the tropics: Impact on atmospheric chemistry and biogeochemical cycles. Science, 250(4988), 1669-1678, (1990).

Crutzen, P. J., A. C. Delany, J. Greenberg, P. Haagenson, L. Heidt, R. Lueb, W. Pollock, Wartburg Seiler, A. Wartburg, and P. Zimmerman. "Tropospheric chemical composition measurements in Brazil during the dry season." Journal of Atmospheric Chemistry 2, no. 3 (1985): 233-256.

Draxler RR, Rolph GD. HySPLIT (Hybrid Single Particle Lagrangian Integrated Trajectory) Model access via NOAA ARL READY website (http://www.arl.noaa.gov/ready/hysplit4.html), NOAA Air Resources Laboratory. *Silver Spring, MD*. 2003.

Eisele, F. L., Mount, G. H., Tanner, D., Jefferson, A., Shetter, R., Harder, J. W., & Williams, E. J. Understanding the production and interconversion of the hydroxyl radical during the Tropospheric OH Photochemistry Experiment. Journal of Geophysical Research: Atmospheres (1984–2012), 102(D5), 6457-6465, (1997).

Fang, S. X., L. X. Zhou, P. P. Tans, P. Ciais, M. Steinbacher, L. Xu, and T. Luan. "In situ measurement of atmospheric CO 2 at the four WMO/GAW stations in China." Atmospheric Chemistry and Physics 14, no. 5 (2014): 2541-2554.

Fang, S. X., P. P. Tans, M. Steinbacher, L. X. Zhou, and T. Luan. "Study of the regional CO2 mole fractions filtering approach at a WMO/GAW regional station in China." Atmospheric Measurement Techniques Discussions 8, no. 7 (2015).

Frankenberg, Christian, Peter Bergamaschi, André Butz, Sander Houweling, Jan Fokke Meirink, Justus Notholt, Anna Katinka Petersen, Hans Schrijver, Thorsten Warneke, and Ilse Aben. "Tropical methane emissions: A revised view from SCIAMACHY onboard ENVISAT." Geophysical Research Letters 35, no. 15 (2008).

Garg, A., Bhattacharya, S., Shukla, P. R., & Dadhwal, V. K. Regional and sectoral assessment of greenhouse gas emissions in India. Atmospheric Environment, 35(15), 2679-2695, (2001).

Gaur, A., Tripathi, S. N., Kanawade, V. P., Tare, V., & Shukla, S. P. Four-year measurements of trace gases (SO2, NOx, CO, and O3) at an urban location, Kanpur, in Northern India. Journal of Atmospheric Chemistry, 71(4), 283-301, (2014).

Gilmanov, T. G., Johnson, D. A., Saliendra, N. Z., Akshalov, K., & Wylie, B. K. Gross primary productivity of the true steppe in Central Asia in relation to NDVI: scaling up CO2 fluxes. Environmental Management, 33(1), S492-S508, (2004).

Goroshi, S. K., Singh, R. P., Panigrahy, S., & Parihar, J. S. Analysis of seasonal variability of vegetation and methane concentration over India using SPOT-VEGETATION and ENVISAT-SCIAMACHY data. Journal of the Indian Society of Remote Sensing, 39(3), 315-321, (2011).

Hassan, A. G. A. Diurnal and Monthly Variations in Atmospheric CO_2 Level in Qena, Upper Egypt. Resources and Environment, 5(2), 59-65, (2015).

Hayashida, S., Ono, A., Yoshizaki, S., Frankenberg, C., Takeuchi, W., & Yan, X. (2013). Methane concentrations over Monsoon Asia as observed by SCIAMACHY: Signals of methane emission from rice cultivation. *Remote Sensing of Environment*, *139*, 246-256.

Huang, J.*, W. Zhang, J. Zuo, J. Bi, J. Shi, X. Wang, Z. Chang, Z. Huang, S. Yang, B. Zhang, G. Wang, G. Feng, J. Yuan, L. Zhang, H. Zuo, S. Wang, C. Fu and J. Chou, 2008: An overview of the Semi-Arid Climate and Environment Research Observatory over the Loess Plateau, Advances in Atmospheric Sciences, 25(6), 1-16.

Huang, J., Yu, H., Guan, X., Wang, G., & Guo, R. (2015). Accelerated dryland expansion under climate change. Nature Climate Change, doi:10.1038/nclimate2837.

Ichoku, C., & Ellison, L. Global top-down smoke-aerosol emissions estimation using satellite fire radiative power measurements. Atmospheric Chemistry and Physics, 14(13), 6643-6667, (2014).

Intergovernmental Panel on Climate Change (IPCC). Climate Change: The IPCC Scientific Assessment, edited by J. T. Houghton, G. J. Jerkins and J. J. Ephraums. Cambridge University Press. New York, (IPCC, 1990).

James, M. E., & Kalluri, S. N. The Pathfinder AVHRR land data set: an improved coarse resolution data set for terrestrial monitoring. International Journal of Remote Sensing, 15(17), 3347-3363, (1994).

Jing, X., Huang, J., Wang, G., Higuchi, K., Bi, J., Sun, Y., ... & Wang, T. (2010). The effects of clouds and aerosols on net ecosystem CO 2 exchange over semi-arid Loess Plateau of Northwest China. *Atmospheric Chemistry and Physics*, *10*(17), 8205-8218.

Jones, C., McConnell, C., Coleman, K., Cox, P., Falloon, P., Jenkinson, D., & Powlson, D. Global climate change and soil carbon stocks; predictions from two contrasting models for the turnover of organic carbon in soil. Global Change Biology, 11(1), 154-166, (2005).

Keppler, F., Hamilton, J. T., Braß, M., & Röckmann, T. Methane emissions from terrestrial plants under aerobic conditions. Nature, 439(7073), 187-191, (2006).

Kim, H. S., Chung, Y. S., Tans, P. P., & Dlugokencky, E. J. Decadal trends of atmospheric methane in East Asia from 1991 to 2013. Air Quality, Atmosphere & Health, 8(3), 293-298, (2015).

King, M. D., Kaufman, Y. J., Menzel, W. P., & Tanre, D. Remote sensing of cloud, aerosol, and water vapor properties from the Moderate Resolution Imaging Spectrometer (MODIS). Geoscience and Remote Sensing, IEEE Transactions on, 30(1), 2-27, (1992).

Kirschke, Stefanie., Bousquet, Philippe., Ciais, Philippe., Saunois, Marielle., Canadell, Josep G., Dlugokencky, Edward J., Bergamaschi, Peter., Bergmann, Daniel., Blake, Donald R., Bruhwiler,

Lori., Cameron-Smith, Philip., Castaldi, Simona., Chevallier, Frédéric., Feng, Liang., Fraser, Annemarie., Heimann, Martin., Hodson, Elke L., Houweling, Sander., Josse, Béatrice., Fraser, Paul J., Krummel, Paul B., Lamarque, Jean-François., Langenfelds, Ray L., Quéré, Corinne Le., Naik, Vaishali., O'Doherty, Simon.,Palmer, Paul I.,Pison, Isabelle.,Plummer, David., Poulter, Benjamin.,Prinn, Ronald G.,Rigby, Matt.,Ringeval, Bruno., Santini,Monia.,Schmidt, Martina.,Shindell, Drew T.,Simpson, Isobel J.,Spahni, Renato.,Steele, L. Paul.,Strode, Sarah A.,Sudo, Kengo.,Szopa, Sophie.,Werf, Guido R. van der.,Voulgarakis, Apostolos., Weele, Michielvan.,Weiss, Ray F.,Williams, Jason E, Guang, Zeng. Three decades of global methane sources and sinks, Nature Geoscience, volume 6, (2013), doi: 10.1038/NGEO1955.

Koshal. A. K. Spatial temporal climatic change variability of cropping system in western Uttar Pradesh, International Journal of Remote Sensing & Geoscience, volume 2, issue 3, (2013).

Lewis, A. C., Evans, M. J., Hopkins, J. R., Punjabi, S., Read, K.A., Purvis, R. M., Andrews, S. J., Moller, S. J., Carpenter, L.J., Lee, J. D., Rickard, A. R., Palmer, P. I., and Parrington, M.: The influence of biomass burning on the global distribution of selected non-methane organic compounds, Atmos. Chem. Phys., 13, 851–867, doi:10.5194/acp-13-851-2013, 2013.

Liu, Yang, Xiufeng Wang, Meng Guo, Hiroshi Tani, Nobuhiro Matsuoka, and Shinji Matsumura. "Spatial and temporal relationships among NDVI, climate factors, and land cover changes in Northeast Asia from 1982 to 2009." GIScience & Remote Sensing 48, no. 3 (2011): 371-393.

Machida, T., K. Kita, Y. Kondo, D. Blake, S. Kawakami, G. Inoue, and T. Ogawa. "Vertical and meridional distributions of the atmospheric CO2 mixing ratio between northern midlatitudes and southern subtropics." Journal of Geophysical Research: Atmospheres (1984–2012) 107, no. D3 (2002): BIB-5.

Mahesh, P., N. Sharma, V. K. Dadhwal, P. V. N. Rao, and B. V. Apparao. "Impact of Land-Sea Breeze and Rainfall on CO2 Variations at a Coastal Station. J Earth Sci Clim Change 5: 201. doi: 10.4172/2157-7617.1000201 Volume 5. Issue 6. (2014).

Mahesh. P, Sreenivas. G, Rao.P.V.N., Dadhwal.V.K.,Sai Krishna. S.V.S. and Mallikarjun. K: High precision surface level CO_2 and CH_4 using Off-Axis Integrated Cavity Output Spectroscopy (OA-ICOS) over Shadnagar, India, International Journal of Remote Sensing, (2015), doi:10.1080/01431161.2015.1104744.

Miller, John B., Luciana V. Gatti, Monica TS d'Amelio, Andrew M. Crotwell, Edward J. Dlugokencky, Peter Bakwin, Paulo Artaxo, and Pieter P. Tans. "Airborne measurements indicate

large methane emissions from the eastern Amazon basin." Geophysical Research Letters 34, no. 10 (2007).

Monastersky, Richard. "Global carbon dioxide levels near worrisome milestone." Nature 497, no. 7447 (2013): 13-14.

Nair, V. S., Moorthy, K. K., Alappattu, D. P., Kunhikrishnan, P. K., George, S., Nair, P. R., & Niranjan, K. (2007). Wintertime aerosol characteristics over the Indo-Gangetic Plain (IGP): Impacts of local boundary layer processes and long-range transport. Journal of Geophysical Research: Atmospheres (1984–2012), 112(D13).

Newman, S., Jeong, S., Fischer, M. L., Xu, X., Haman, C. L., Lefer, B., Alvarez, S.,Rappenglueck, B.,Kort, E. A., Andrews, A. E., Peischl, J.,Gurney, K. R.,Miller, C. E.,and Yung, Y. L.,: Diurnal tracking of anthropogenic CO_2 emissions in the Los Angeles basin megacity during spring, Atmos. Chem. Phys., 13, 4359–4372, 2013, doi:10.5194/acp-13-4359-2013.

Nishanth, T., K. M. Praseed, M. K. Satheesh Kumar, and K. T. Valsaraj. "Observational study of surface O3, NOx, CH4 and total NMHCs at Kannur, India." Aerosol. Air. Qual. Res 14 (2014): 1074-1088.

Pan, X. L., Kanaya, Y., Wang, Z. F., Liu, Y., Pochanart, P., Akimoto, H., Sun, Y. L., Dong, H. B., Li, J., Irie, H., and Takigawa, M.: Correlation of black carbon aerosol and carbon monoxide in the high-altitude environment of Mt. Huang in Eastern China, Atmos. Chem. Phys., 11, 9735-9747, doi:10.5194/acp-11-9735-2011, 2011

Paul, J. B., Lapson, L., & Anderson, J. G.. Ultrasensitive absorption spectroscopy with a high-finesse optical cavity and off-axis alignment. Applied Optics, 40(27), 4904-4910, (2001).

Patil, M. N., T. Dharmaraj, R. T. Waghmare, T. V. Prabha, and J. R. Kulkarni. "Measurements of carbon dioxide and heat fluxes during monsoon-2011 season over rural site of India by eddy covariance technique." Journal of Earth System Science 123, no. 1 (2014): 177-185.

Pielke, Roger A., Gregg Marland, Richard A. Betts, Thomas N. Chase, Joseph L. Eastman, John O. Niles, and Steven W. Running. "The influence of land-use change and landscape dynamics on the climate system: relevance to climate-change policy beyond the radiative effect of greenhouse gases." Philosophical Transactions of the Royal Society of London A: Mathematical, Physical and Engineering Sciences 360, no. 1797 (2002): 1705-1719.

Ramachandran, S., and T. A. Rajesh. "Black carbon aerosol mass concentrations over Ahmedabad, an urban location in western India: comparison with urban sites in Asia, Europe, Canada, and the United States." Journal of Geophysical Research: Atmospheres (1984–2012) 112, no. D6 (2007).
Salomonson, Vincent V., W. L. Barnes, Peter W. Maymon, Harry E. Montgomery, and Harvey Ostrow. "MODIS: Advanced facility instrument for studies of the Earth as a system." Geoscience and Remote Sensing, IEEE Transactions on 27, no. 2 (1989): 145-153.

637 Smith, K. A., Ball, T., Conen, F., Dobbie, K. E., Massheder, J., & Rey, A. Exchange of greenhouse
638 gases between soil and atmosphere: interactions of soil physical factors and biological processes.
639 European Journal of Soil Science, 54(4), 779-791, (2003).

640 Schneising, O., M. Buchwitz, J. P. Burrows, H. Bovensmann, P. Bergamaschi, and W. Peters.
641 "Three years of greenhouse gas column-averaged dry air mole fractions retrieved from satellite–
642 Part 2: Methane." Atmos. Chem. Phys 9, no. 2 (2009): 443-465.

643 Sharma Neerja, Dadhwal, V.K., Kant, Y., Mahesh, P., Mallikarjun, K., Gadavi, Harish, Sharma,
644 Anand., Ali, M.M. Atmospheric CO_2 Variations in Two Contrasting Environmental Sites Over
645 India. Air, Soil and Water Research 2014:7 61–68, (2014), doi:10.4137/ASWR.S13987.

646 Sharma, Anu Rani, Shailesh Kumar Kharol, K. V. S. Badarinath, and Darshan Singh. "Impact of
647 agriculture crop residue burning on atmospheric aerosol loading—a study over Punjab State,
648 India." In Annales geophysicae: atmospheres, hydrospheres and space sciences, vol. 28, no. 2, p.
649 367. 2010.

650 Sharma, Neerja, Rabindra K. Nayak, Vinay K. Dadhwal, Yogesh Kant, and Meer M. Ali.
651 "Temporal variations of atmospheric CO_2 in Dehradun, India during 2009." Air, Soil and Water
652 Research 6 (2013): 37.

653 Stocker, T.F., Qin, D., Plattner, G.K., Alexander, L.V., Allen, S.K., Bindoff, N.L., Bréon, F.M., Church,
654 J.A., Cubasch, U., Emori, S., Forster, P., Friedlingstein, P., Gillett, N., Gregory, J.M., Hartmann, D.L.,
655 Jansen, E., Kirtman, B., Knutti, R., Krishna Kumar, K., Lemke, P., Marotzke, J., Masson-Delmotte, V.,
656 Meehl, G.A., Mokhov, I.I., Piao, S., Ramaswamy, V., Randall, D., Rhein, M., Rojas, M., Sabine, C.,
657 Shindell, D., Talley, L.D., Vaughan D.G., and Xie, S.P. Technical Summary. In: Climate Change 2013:
658 The Physical Science Basis. Contribution of Working Group I to the Fifth Assessment Report of the
659 Intergovernmental Panel on Climate Change [Stocker, T.F., D. Qin, G.-K. Plattner, M. Tignor, S.K. Allen,
660 J. Boschung, A. Nauels, Y. Xia, V. Bex and P.M. Midgley (eds.)]. Cambridge University Press, Cambridge,
661 United Kingdom and New York, NY, USA, (2013).Shea, S.J.O, G. Allen1, M. W. Gallagher, S. J.-B.
662 Bauguitte, S. M. Illingworth, M. Le Breton, J. B. A. Muller,C. J. Percival, A. T. Archibald, D. E.
663 Oram, M. Parrington,*, P. I. Palmer, and A. C. Lewis. Airborne observations of trace gases over
664 boreal Canada during BORTAS: campaign climatology, air mass analysis and enhancement ratios.
665 Atmos. Chem. Phys., 13, 12451–12467, 2013 atmos-chem-phys.net/13/12451/2013/
666 doi:10.5194/acp-13-12451-2013

667 Stohl, Andreas, Markus Hittenberger, and Gerhard Wotawa. "Validation of the Lagrangian particle
668 dispersion model FLEXPART against large-scale tracer experiment data." Atmospheric
669 Environment 32, no. 24 (1998): 4245-4264.

670

671 Stull, R. B. (1988). Similarity theory. In *An Introduction to Boundary Layer Meteorology* (pp.
672 347-404). Springer Netherlands.

673 Taylor J. An Introduction to Error Analysis: The Study of Uncertainties in Physical Measurement,
674 University Science Books, And ISBN: 093570275X (ISBN13: 9780935702750), (1997).

675 Thum, T., T. Aalto, T. Laurila, M. Aurela, J. Hatakka, Anders Lindroth, and T. Vesala. "Spring
676 initiation and autumn cessation of boreal coniferous forest CO2 exchange assessed by
677 meteorological and biological variables." Tellus B 61, no. 5 (2009): 701-717.

678 Tohjima, Y., Kubo, M., Minejima, C., Mukai, H., Tanimoto, H., Ganshin, A., Maksyutov, S.,
679 Katsumata, K., Machida, T., and Kita, K.: Temporal changes in the emissions of CH4 and CO
680 from China estimated from CH4 / CO2 and CO / CO2 correlations observed at Hateruma Island,
681 Atmos. Chem. Phys., 14, 1663-1677, doi:10.5194/acp-14-1663-2014, 2014.

682
683 Vaghjiani, Ghanshyam L., and A. R. Ravishankara. "New measurement of the rate coefficient for
684 the reaction of OH with methane." Nature 350, no. 6317 (1991): 406-409.

685 Wang, B-R., X-Y. Liu, and J-K. Wang. "Assessment of COSMIC radio occultation retrieval
686 product using global radiosonde data." Atmospheric Measurement Techniques 6, no. 4 (2013):
687 1073-1083.

688 Wang, G., J. Huang*, W. Guo, J. Zuo, J. Wang, J. Bi, Z. Huang, and J. Shi, 2010: Observation
689 analysis of land-atmosphere interactions over the Loess Plateau of northwest China, J. Geophys.
690 Res., 115, D00K17,doi:10.1029/2009JD013372.

691 Worthy, Douglas EJ, Elton Chan, Misa Ishizawa, Douglas Chan, Christian Poss, Edward J.
692 Dlugokencky, Shamil Maksyutov, and Ingeborg Levin. "Decreasing anthropogenic methane
693 emissions in Europe and Siberia inferred from continuous carbon dioxide and methane
694 observations at Alert, Canada." Journal of Geophysical Research: Atmospheres (1984–2012) 114,
695 no. D10 (2009).

696 Yunck, Thomas P., Liu Chao-Han, and Randolph Ware. "A history of GPS sounding." Terrestrial
697 Atmospheric and Oceanic Sciences 11, no. 1 (2000): 1-20.

698

699

700

701

702

703

704

705

Table 1 Data used

Sensor	Period	Parameter	resolution	Source
GGA-24EP	Jan-2014 to Dec 2014	CO_2,CH_4 and H_2O	1 Hz time	ASL,NRSC
42*i*-NO-NO_2-NO_x	Jul-2014 to Sep-2014	NOx(=NO+NO_2)	1 min time	ASL,NRSC
49i-O_3	Jul-2014 to Sep-2014	O_3	1 min time	ASL,NRSC
AWS	Jan-2014 to Dec-2014	WS,WD,AT,RH	60 min time	NRSC
Terra/MODIS	Jan-2014 to Dec-2014	NDVI	5 Km horizontal	http://ladsweb.nascom.nasa.gov/data/search.html
COSMIC-1DVAR	Jul-2013 to Jun-2014	Refractivity (N)	0.1 Km vertical	
HYSPLIT	Jan-2014 to Dec-2014	Backward trajectory	5 day isentropic model (1km to 4 km)	http://ww.arl.noaa.gov/ready/hysplit4.html]
FEER v1	Jan-2013 to Dec-2013	fire radiative power (FRP)		http://ladsweb.nascom.nasa.gov/data/search.html

Table 2 Statistical correlation between CO_2 and CH_4

S.No	**Seasons**	**Correlation coefficient (R)**	**Slope** $(\frac{Y_{CH4}\,(ppm)}{X_{CO2}(ppm)})$	ψ_{slope} **(ppm)**	$\Psi_{y\text{-}int}$ **(ppm)**
1	Monsoon (JJAS)	0.61	0.005	0.00015	1.91
2	Post-monsoon (OND)	0.72	0.0065	0.00014	1.52
3	Winter (JF)	0.80	0.0085	0.00018	9.13
4	Pre-monsoon (MAM)	0.80	0.0059	0.00021	2.73

721 **Table 3** Seasonal amplitudes of CO_2 and CH_4 over study region arriving from different directions

722

Wind Direction	Winter $\frac{CO_2}{CH_4}$ (ppm)	Pre-monsoon $\frac{CO_2}{CH_4}$ (ppm)	Monsoon $\frac{CO_2}{CH_4}$ (ppm)	Post-monsoon $\frac{CO_2}{CH_4}$ (ppm)
0-45	399.85/1.98	410.37/1.94	400.72/1.91	395.13/2.02
45-90	391.66/1.94	399.59/1.89	388.82/1.91	390.23/1.98
90-135	391.57/1.93	397.79/1.87	388.99/1.87	389.06/1.97
135-180	389.34/1.89	393.87/1.85	391.81/1.86	387.69/1.97
180-225	391.14/1.89	396.75/1.85	390.28/1.82	392.30/2.02
225-270	389.13/1.88	394.81/1.86	390.26/1.82	384.40/1.94
270-315	388.68/1.87	398.68/1.89	389.58/1.82	384.99/1.93
315-360	390.87/1.91	401.17/1.89	387.58/1.83	389.32/1.98

723

724 **Table 4** Cluster analysis of air mass trajectories reaching Shadnagar at various heights during different
725 seasons

726

Seasonal Backward trajectory (%)	NW				NE				SE				SW			
	1 km	2 km	3 km	4 km	1 km	2 km	3 km	4 km	1 km	2 km	3 km	4 km	1 km	2 km	3 km	4 km
Winter	54	32	2	0	32	24	44	52	10	25	11	7	4	19	42	41
Pre-monsoon	24	9	8	1	26	31	64	78	36	46	2	10	14	14	26	11
Monsoon	0	1	7	19	12	34	80	70	4	4	4	6	84	61	9	5
Post-monsoon	42	15	11	14	47	53	41	49	8	30	32	26	3	2	16	11

727

728

729

730

731

732

733

734

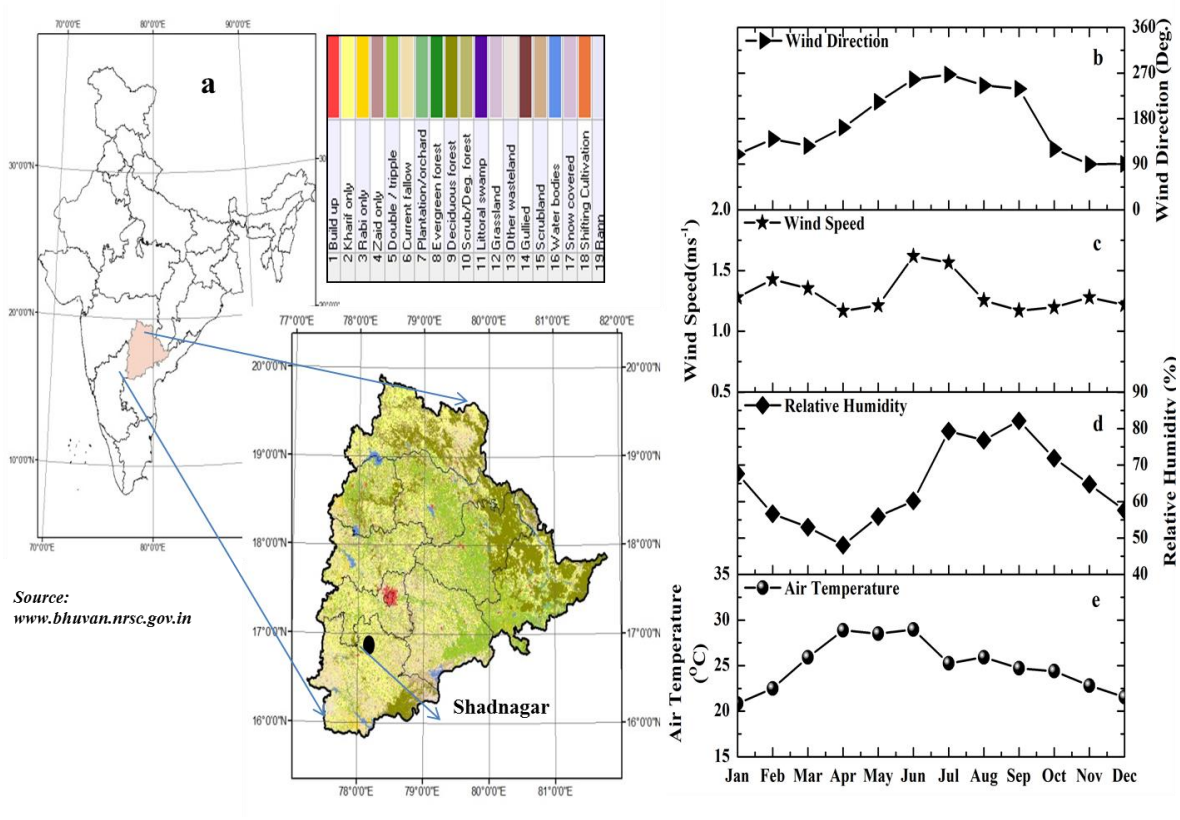

Figure 1 a) Schematic representation of study area; b-e) Seasonal variation of prevailing meteorological conditions during 2014

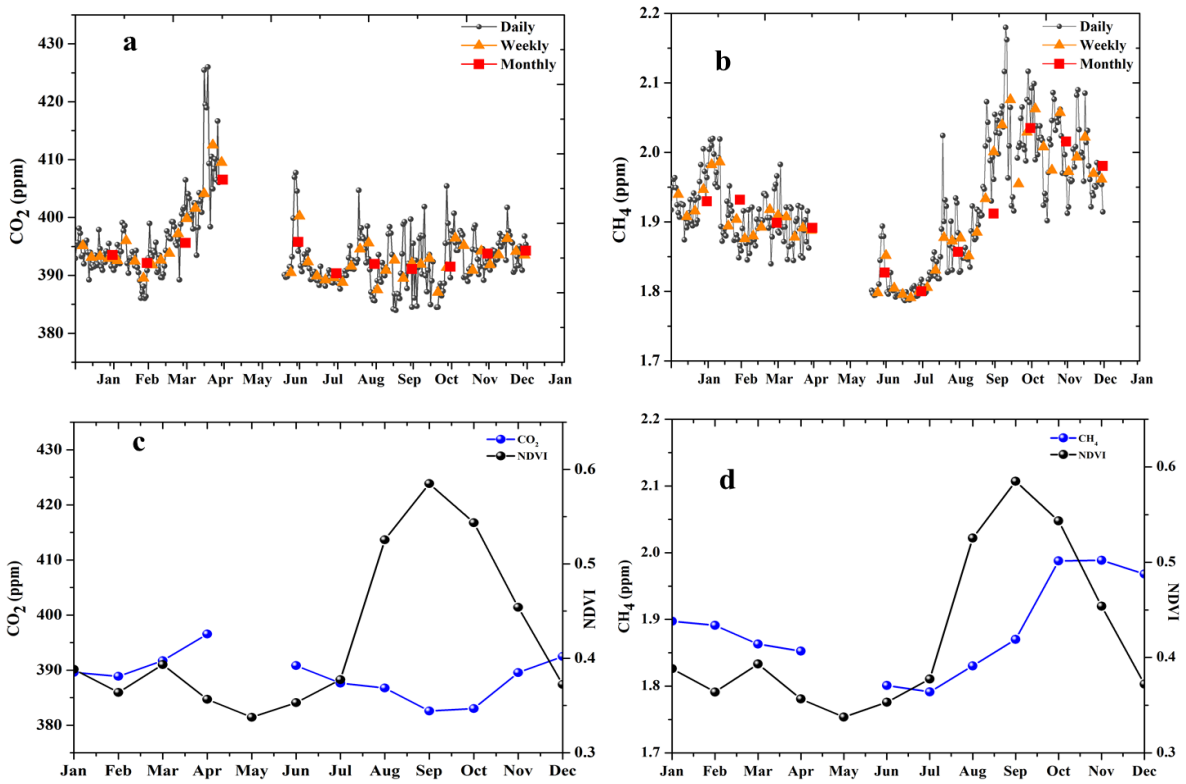

752

753 **Figure 2** a-b) Temporal variations of CO_2 and CH_4; c-d) Seasonal variations of CO_2 and CH_4 in conjunction
754 with NDVI (Normalized Difference Vegetation Index)during 2014

755

756

757

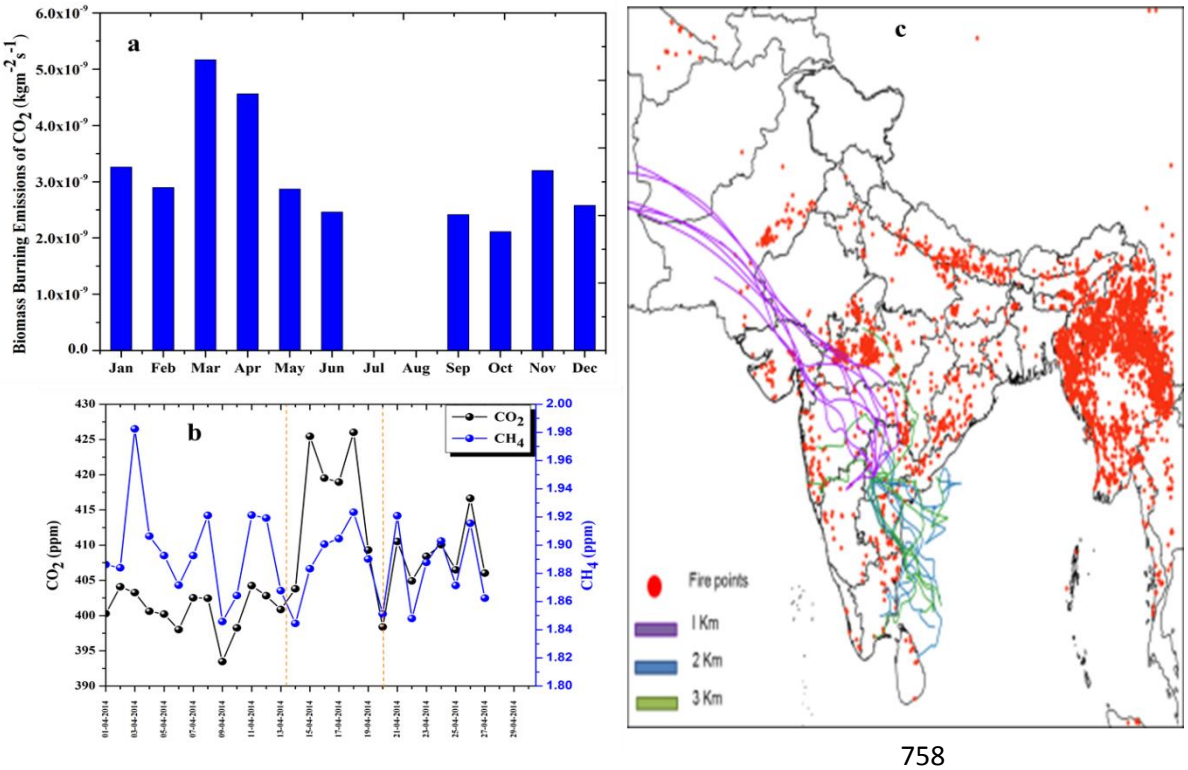

758

759 **Figure 3** a) Long term analysis of CO_2 biomass burning emissions over study region b) Biomass signatures
760 on CO_2/CH_4 during 14-21 April 2014, a case study c) Spatial distribution of MODIS derived fire counts
761 over Indian region during 14-21 April 2014.

762
763
764
765
766
767
768
769
770
771
772
773
774
775

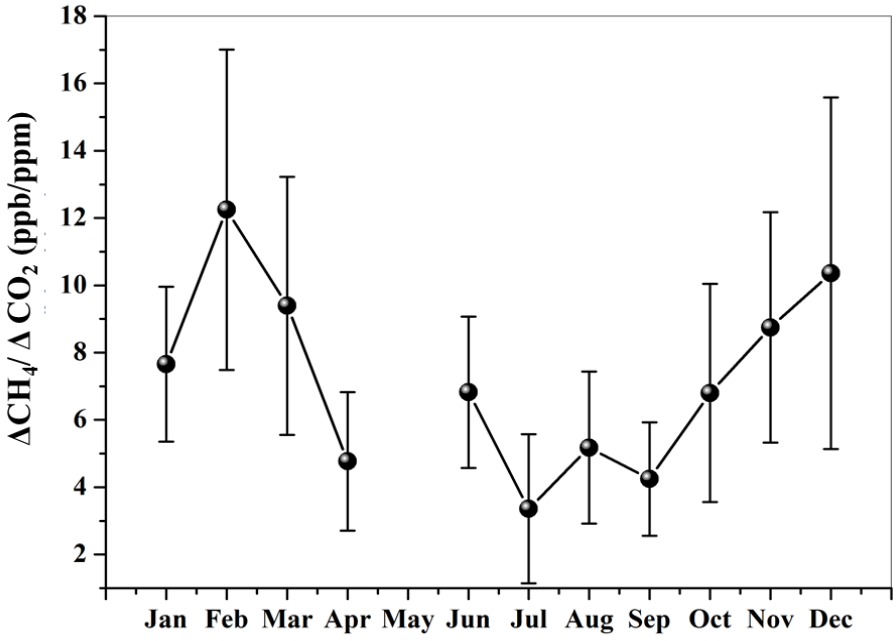

776 **Figure 4** Monthly variation of $\Delta CH_4/\Delta CO_2$ during study period

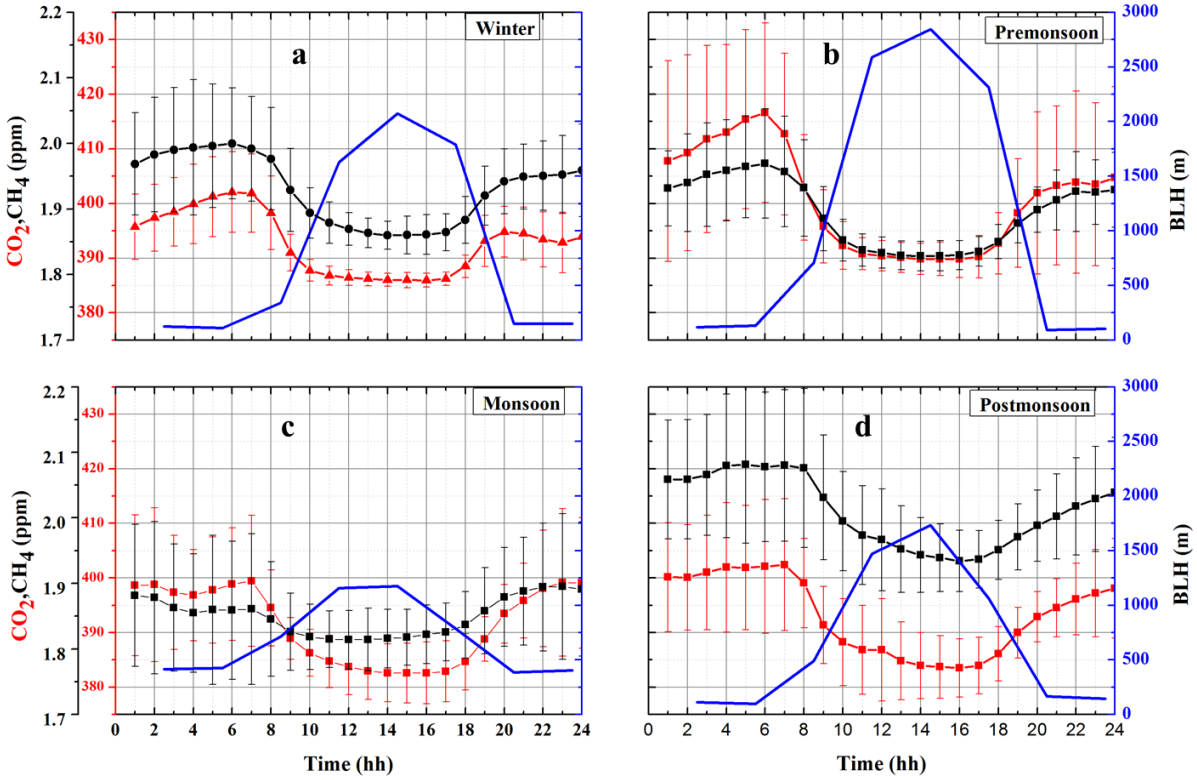

777 Figure 5 a-d) Seasonal variations of diurnal averaged CO_2/CH_4 against boundary layer height during 2014

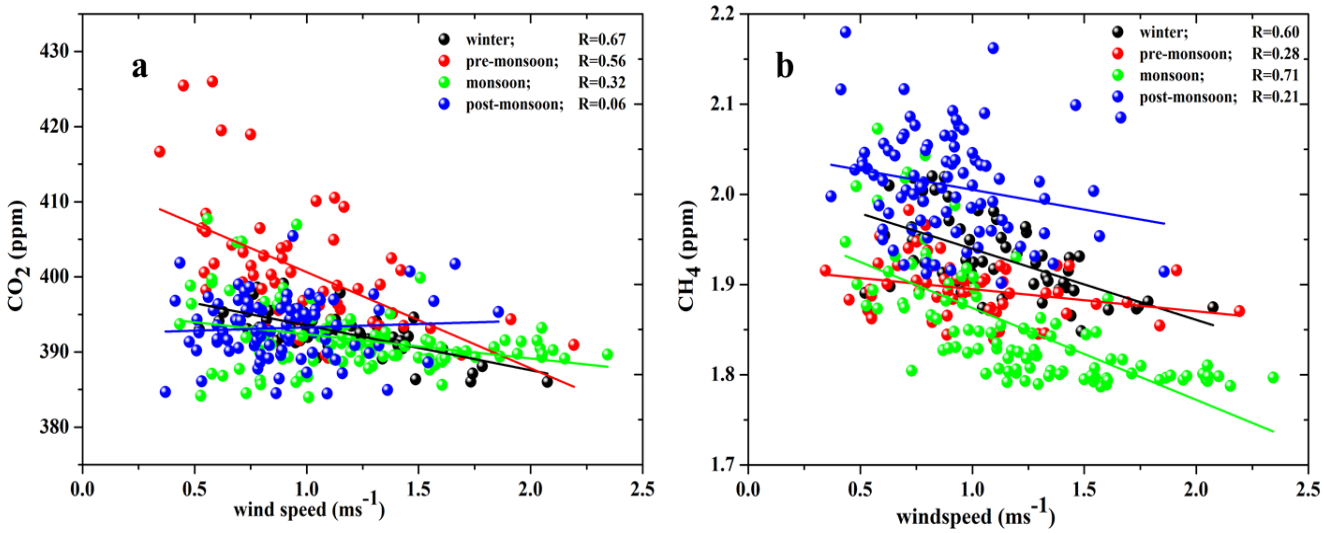

778

779 Figure 6 a-b) Daily mean scatterplot between wind speed and GHGs (CO_2 and CH_4).

780

781

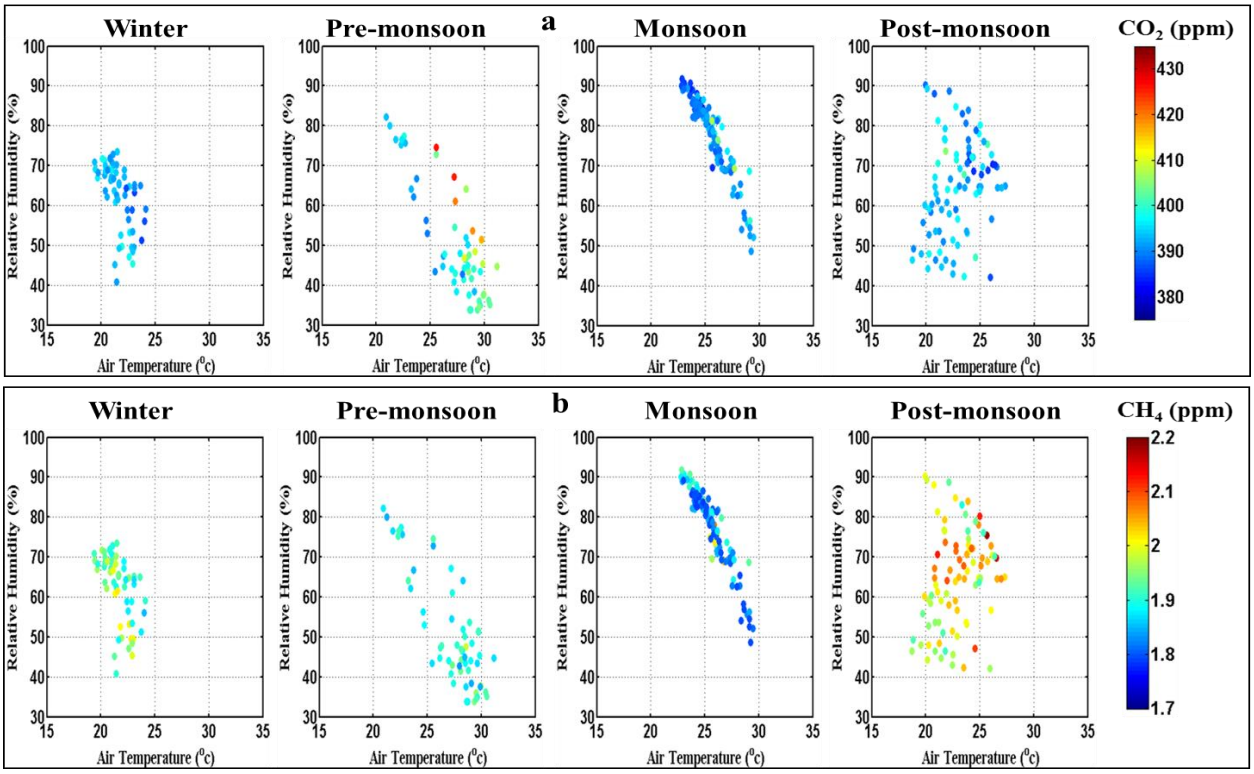

Figure 7 a-b) Daily mean seasonal variation of CO_2 and CH_4 as function of humidity and air temperature during 2014

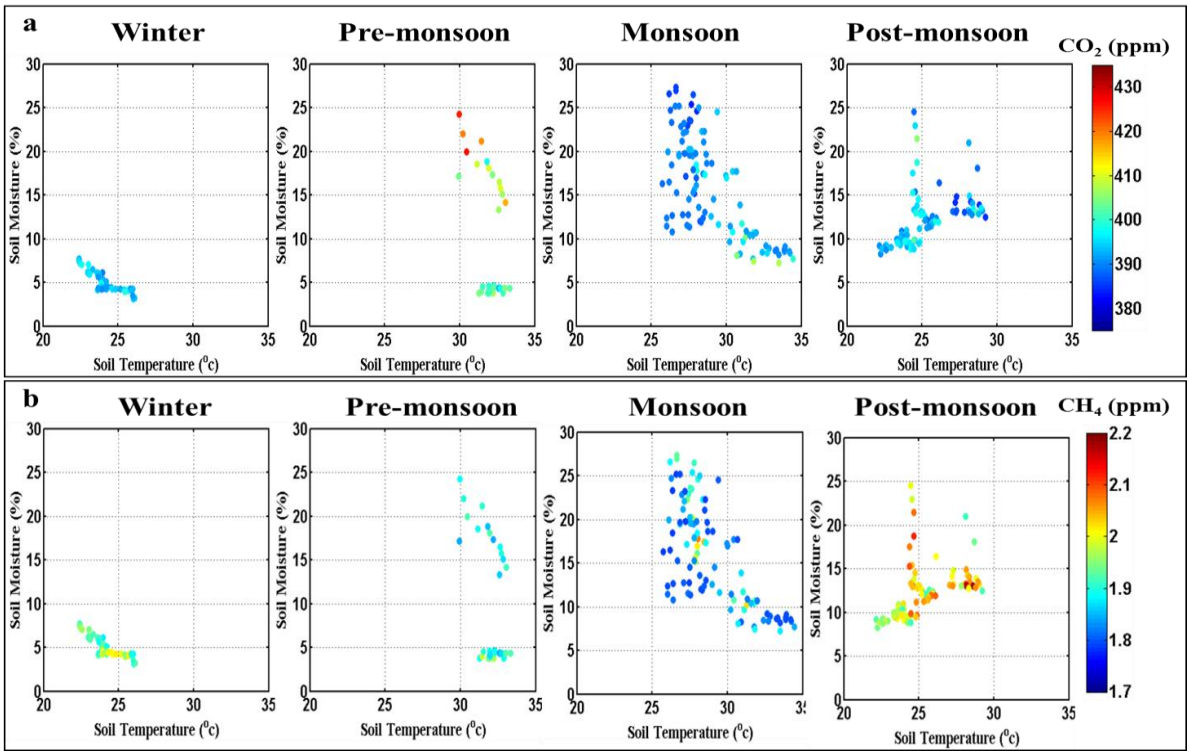

Figure 8 a-b) Daily mean seasonal variation of CO_2 and CH_4 as function of soil temperature and soil moisture during 2014

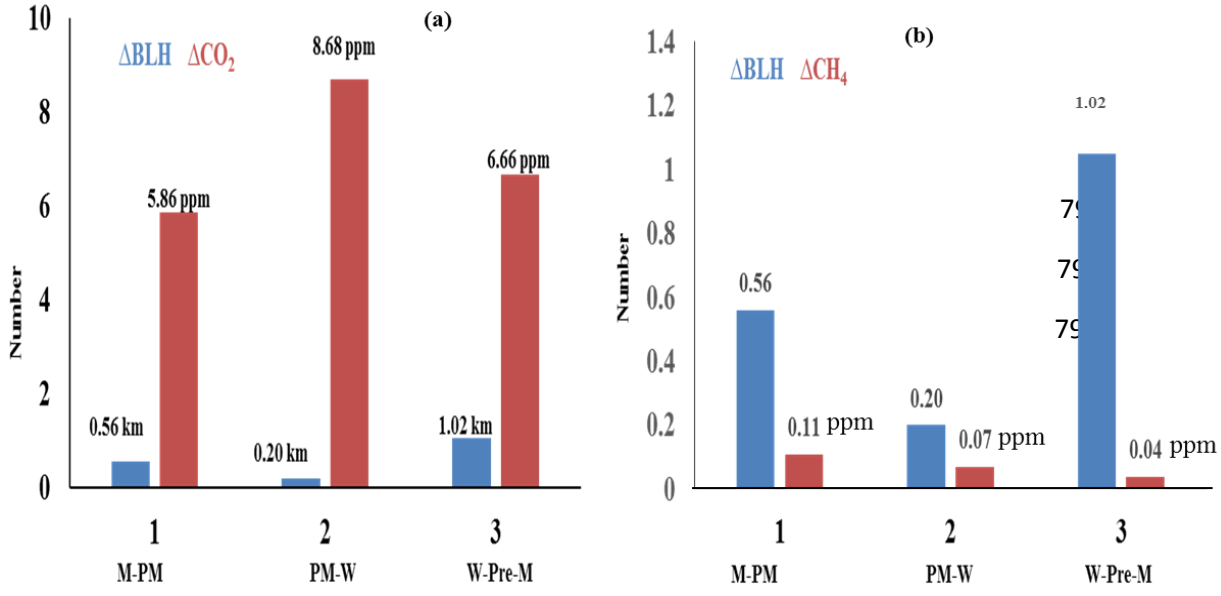

Figure 9 Seasonal difference in BLH against respective change in a) CO_2 and b) CH_4

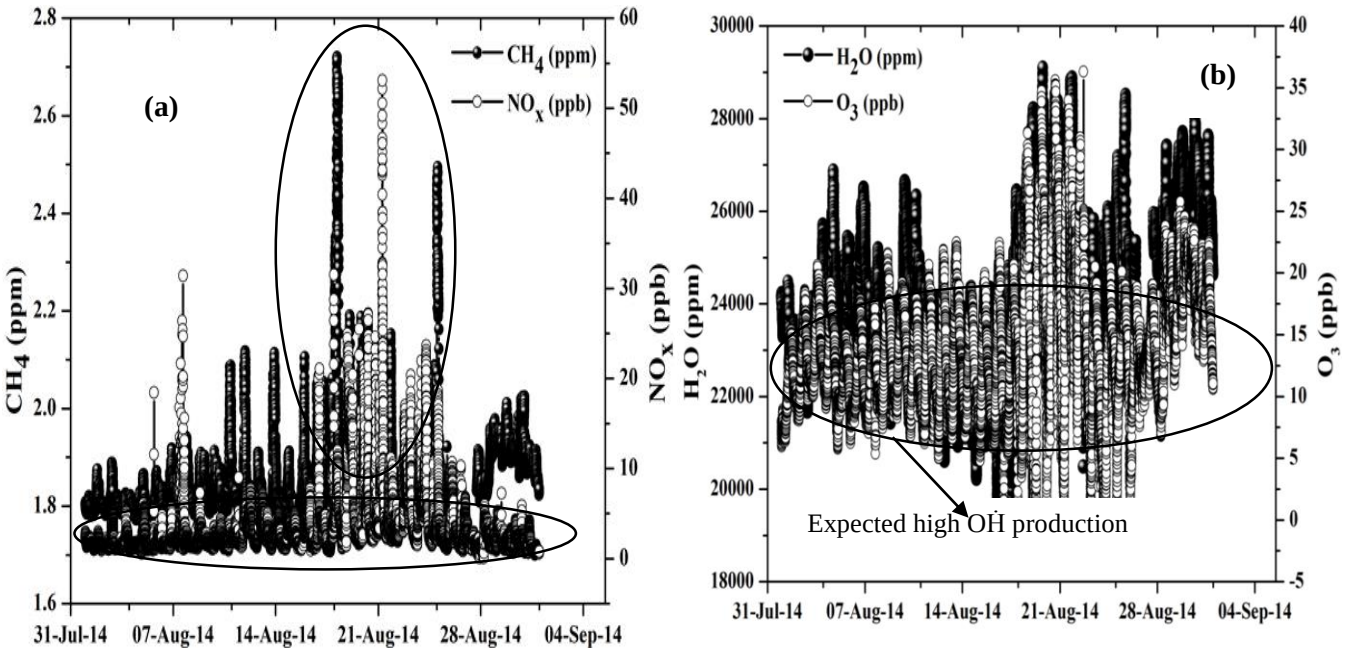

Figure 10 Time series analysis of a) CH_4 vs. NO_x, b) H_2O vs. O_3

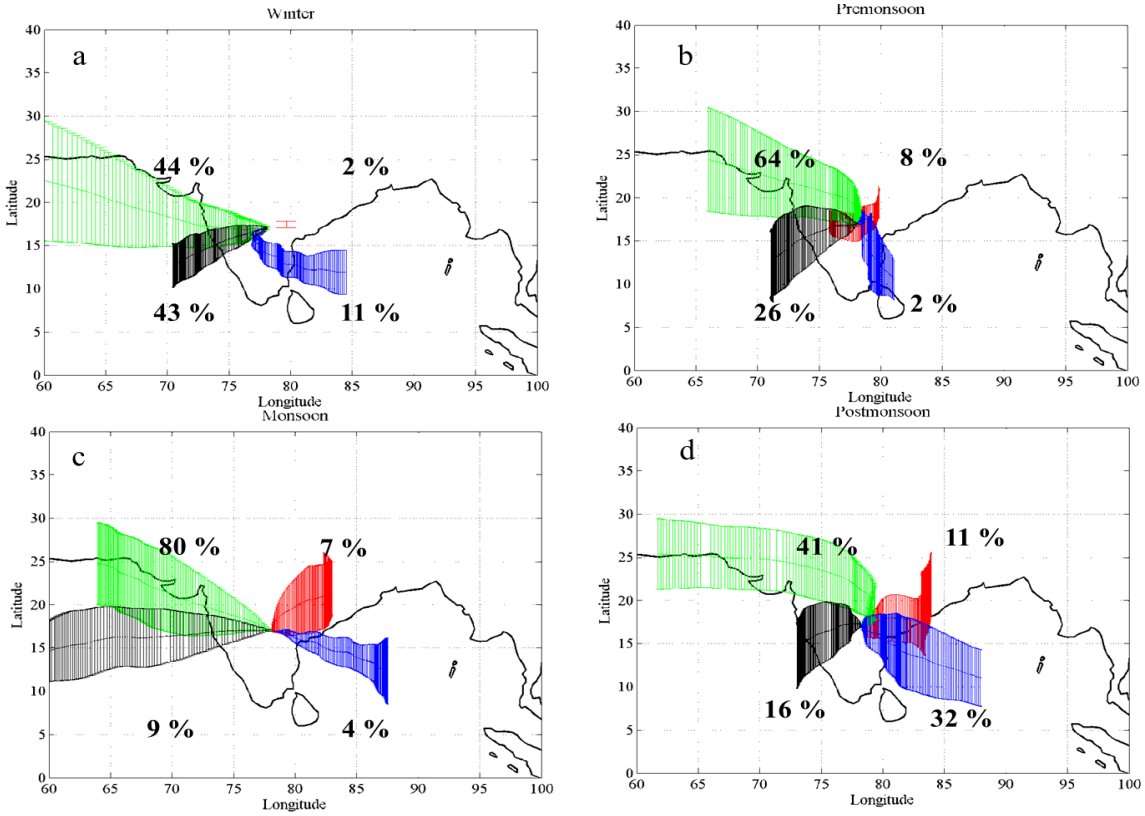

Figure 11 a-d) Long range circulation of air mass trajectories ending over Shadnagar at 3 km during winter, pre-monsoon, monsoon and post-monsoon